Spectroscopic evaluation of thermodynamics of trivalent actinides in brines

Th. Fanghänel[*], J.-I. Kim

Forschungszentrum Karlsruhe, Institut für Nukleare Entsorgungstechnik, Postfach 3640, D-76021 Karlsruhe, Germany

Abstract

A systematic investigation of thermodynamic properties of trivalent aquatic actinides has been initiated in our laboratory to develop models capable of predicting their behavior in natural multicomponent brines of high concentration. An overview on this subject is provided taking curium as a representative for trivalent actinides. Cm(III) is chosen, because of its high fluorescence spectroscopic sensitivity that enables a direct speciation in solution in the nanomolar concentration range. Interactions of Cm(III) with the main natural inorganic ligands Cl^-, SO_4^{2-}, OH^- and CO_3^{2-} are investigated by time resolved laser fluorescence spectroscopy (TRLFS). An overall thermodynamic model for trivalent actinides is developed based on the ion interaction (Pitzer) approach. © 1998 Elsevier Science S.A.

1. Introduction

The option of nuclear waste disposal in a salt formation has attracted our attention to the aquatic chemistry and thermodynamics of actinides in concentrated electrolyte solutions. Therefore, a systematic investigation of thermodynamic properties of trivalent aquatic actinides has been initiated in our laboratory. The aim of the work is to develop models capable of predicting their behavior in natural multicomponent brines of high concentration. For predicting the mobility of actinides in repository systems a variety of coupled processes has to be taken into account. To know the stability and distribution of the actinide species in the aqueous phase as a function of several key variables (e.g. pH, chemical composition, temperature etc.) is an essential prerequisite for the quantification of these processes and is thus the basis for the modeling of the migration behavior of actinides in natural aquatic systems. For this purpose a thermodynamic equilibrium concept is applied, which entails the following quantities at given temperature (pressure):

- chemical potentials μ_i° of all species (thermodynamic equilibrium constants)
- activity coefficients γ_i of all species as a function of the solution composition.

In brines, trivalent actinides form a variety of complexes with inorganic ligands. Potential inorganic ligands are: OH^-, CO_3^{2-}, $H_2PO_4^-$, $H_3SiO_4^-$, F^-, HCO_3^-, SO_4^{2-}, Cl^-.

A number of experimental techniques have been applied for the determination of the complex formation equilibria of trivalent actinides in aqueous solutions, e.g. solubility measurements [1–7], solvent extraction [8,9], and spectroscopic methods [5,10]. The available experimental data for one of the most important and extensively investigated trivalent actinides — Am(III) — are summarized and critically evaluated in the recently published NEA Thermodynamic Database [11]. Available literature data until 1992 on the complexation of Cm(III) with inorganic ligands are compiled by Fuger et al. [12] and discussed in detail in our previous publications [13–17]. With a few exceptions the experimental investigation on the aqueous chemistry and thermodynamics of trivalent actinides have been performed in non-complexing electrolytes, usually $NaClO_4$ solutions of limited ionic strength. Those data do not in general allow to predict the behavior of trivalent actinides in concentrated brines of the sea water system (Na-K-Mg-Ca-Cl-SO_4). Moreover the available data scatter very often several orders of magnitude.

Among the different experimental techniques applied for the quantification of thermodynamic data, spectroscopic methods have the advantage that the speciation information can be derived directly. However the limited sensitivity of UV-absorption spectroscopy allows the speciation in a limited concentration range which is in many systems above the solubility limit of trivalent actinides. New laser spectroscopic techniques, e.g. laser-induced photoacoustic spectroscopy (LPAS) [18] and time resolved laser fluores-

[*]Corresponding author. Fax: +49 7247 825994; e-mail: thomas@ine.fzk.de

cence spectroscopy (TRLFS) [19,20] with considerably higher speciation sensitivity have been applied to overcome such shortcomings. In particular the high fluorescence spectroscopic sensitivity of TRLFS enables the speciation of Cm(III) in the nanomolar concentration range which is considerably below the solubility limit of Cm(III) solid phases. We have therefore applied TRLFS to study systematically the behavior of Cm(III) as a representative for trivalent actinides in diluted to saturated NaCl solutions.

Using the spectroscopic results an overall thermodynamic model for trivalent actinides is developed. The model is based on the ion interaction (Pitzer) approach [21], which is at present the best suited semiempirical approach for describing activity coefficients of different species up to the high ionic strength of natural brines. The paper summarizes the present state of knowledge on the aquatic chemistry and thermodynamics of Cm(III) in concentrated electrolyte solutions.

2. Spectroscopic characteristics of Cm

The spectroscopic characteristics of Cm(III) are discussed in detail in ref. [20] and in the references therein. A brief summary is presented in the following.

2.1. Fluorescence emission of Cm(III)

A simplified term scheme of Cm(III) including the important excitation and emission states is illustrated in Fig. 1. The groundstate of the half filled $5f^7$ configuration exhibits only a small splitting of few wavenumbers. Therefore, for practical purposes, transitions from and to the groundstate involve a single level. Excitations to the F, G and H states are the main absorption bands with maxima for the non-complexed Cm^{3+} aquo ion at 396.0 nm ($\varepsilon=$ 55.3), 381.3 nm ($\varepsilon=32.6$), and 375.5 nm ($\varepsilon=29.3$ 1/mol cm) [22]. In solution at room temperature fluorescence

Fig. 1. Schematic energy levels and spectroscopic characteristics of Cm(III).

emission is observed only from the A-state to the ground-state Z. A relatively broad unresolved emission band (FWHM=8.3 nm) is observed for the aqueous Cm^{3+} ion at room temperature. The emission bands of inner-sphere complexes of Cm(III) with inorganic ligands are shifted several nm to the red side relative to the emission spectrum of the aqueous Cm^{3+} ion.

2.2. Excitation of Cm(III)

Excitation spectra obtained by scanning the excitation wavelength and monitoring the emitted light within a constant wavelength range are usually equivalent to absorption spectra. Complexation causes a shift of the excitation bands of about 2–3 nm to the red. However, excitation spectra are usually less selective on complexation than emission spectra. Hence the information contained in the latter is in general utilized for the quantification of complexation equilibria.

2.3. Lifetime (fluorescence decay) of Cm(III)

Fluorescence decay rates are caused by radiative and non-radiative processes. The radiative decay rate is related to the transition probability. For the A→Z transition of Cm^{3+} in 1 M $HClO_4$ the decay rate is calculated to be 770 s^{-1} [23], which corresponds to a radiative lifetime (reciprocal decay rate) of 1.3 ms. Non-radiative decay is due mainly to energy transfer from the excited state to ligand vibrators, e.g. OH vibration of coordinated H_2O molecules. A lifetime of 65 μs is determined for the aqueous Cm^{3+} ion [13,16,19,24], while in D_2O the lifetime is increased to 1270 μs [25] which is close to the above calculated radiative lifetime.

A linear correlation is attained between the decay rate (reciprocal life time of the excited state) and the number of H_2O molecules in the first coordination sphere of Cm(III) complexes [25]. Based on this correlation structural information is gained from experimentally determined lifetimes of various Cm species.

The time dependence of the Cm(III) fluorescence emission in mixed solutions of different Cm(III) species contains information on the kinetics of the complexation reaction. Two limiting states can be discussed.

1. The ligand exchange reaction rate is high compared to the fluorescence decay rate of the excited Cm(III). Under these conditions, differences in absorptivity at the excitation wavelength and in the fluorescence decay rate of the different species are averaged, as the species distribution is governed by the thermodynamic equilibrium. A monoexponential decay law
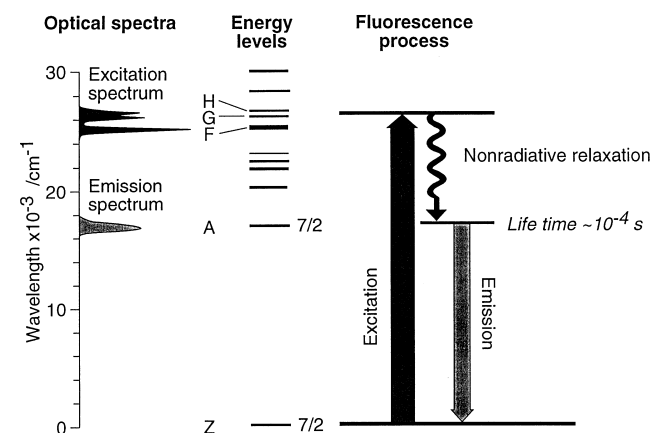
$$I = I° e^{-t/\tau_{av}}$$

(I, intensity at time t, $I°$, intensity at $t = 0$, τ_{av}, average lifetime) with an average lifetime of the species in equilibrium is expected [17].

2. The ligand exchange rate is low in comparison to the fluorescence decay rate of the excited Cm(III). The decay of the individual (excited) Cm(III) species is indicated in a deviation of the time dependence of the fluorescence emission from a monoexponential decay law

$$I = I_1°x_1e^{-t/\tau_1} + I_2°x_2e^{-t/\tau_2} + \dots$$

The monoexponential decay behavior observed for the inorganic Cm(III) complexes discussed in this contribution, indicate a high ligand exchange rate for the complexation equilibria. A typical example is discussed for sulfate complexes of Cm(III) (see below).

3. Experimental set-up

Detailed descriptions on the experimental set-up and the experimental procedures are given elsewhere [13,15–17,26]. For excitation, an excimer-pumped dye laser (Lambda Physics, EMG 201 and FL 3002) emitting at 375 nm is used. The laser light (pulse energy about 10 mJ at 10 Hz repetition rate) is coupled by a 450 μm Ø quartz fiber into a glove box. The emitted light is collected by a fiber bundle and directed to a polychromator (Jabin Yvon, HR320). The dispersed light is detected by an optical multichannel analyzer (Spectroscopy Instr., ST180, IRY 700 G). Time resolution is performed by a gated microchannelplate. For spectroscopic studies at elevated pressure a special cell was constructed using fiber optics, which can be used up to 20 bar and 200°C.

4. Data evaluation methodology

The thermodynamic equilibrium constant $\beta°$ for a complexation reaction is given by:

$$\beta^0 = \frac{\gamma_{CmL}}{\gamma_{Cm}\gamma_L^n} \frac{[CmL_n]}{[Cm^{3+}][L]^n} = \frac{\gamma_{CmL}}{\gamma_{Cm}\gamma_L^n}\beta \tag{1}$$

In order to establish the chemical model, emission spectra of traces of Cm(III) are measured in solutions of a background electrolyte with constant and relatively high ionic strength with varying ligand concentrations. The high and constant ionic strength is a prerequisite for keeping the activity coefficients of the trace components constant.

Considering the change of the emission spectra measured at different ligand concentrations the stability of different curium species is postulated. Spectra of the pure species are derived either by direct measurement (e.g. Cm^{3+} is the major Cm(III) species at low pH) or by deconvolution of mixed spectra. The fractions of each

species are deduced from the spectra by peak deconvolution. A typical example is illustrated for the hydrolysis of Cm(III) (see below).

In order to verify the postulated species in equilibrium, Eq. (1) is rearranged to

$$\log([CmL_n]/[Cm^{3+}]) = \log\beta + n\log[L] \tag{2}$$

As the activity coefficients are constant, log β (apparent stability constant) is defined to be $\log \beta° - \log \prod \gamma_i$. When $\log ([CmL_n]/[Cm^{3+}])$ is plotted as a function of log [L], straight lines with slopes n confirm the initial postulation. An example is illustrated for the formation of sulfato complexes (see below) [17].

This procedure is easily applicable for the formation of strong complexes. If weak complexes are formed the ligand concentration has to be increased up to values which do not allow us to keep the activity coefficients of reactants and products constant. Hence the dependence of the activity coefficients on the ligand concentration has to be taken into consideration for the evaluation. This complicates the evaluation procedure considerably and causes higher uncertainties in the derived thermodynamic constants. The problem is illustrated for the formation of sulfato complexes (see below).

In a second step the ligand concentration is kept constant at an optimal value ($CmL_n \sim CmL_{n+1}$) and the brine composition (e.g. NaCl-molality) is varied systematically from low concentration to saturation. In this way the activity coefficients of the trace components are determined. $\gamma(CmL_n) = f(m_{NaCl})$ and $\beta°$ are simultaneously evaluated by taking into account the activity coefficients of the aqueous Cm^{3+} ion and ligand. The activity coefficients are finally used to derive the ion interaction parameters of the Pitzer approach.

5. Results and discussion

5.1. Cm(III)-chloro-complexes

Although the Cm(III) chloro complexes are expected to be very weak, they might be important in brines with very high Cl^- concentrations ($m_{Cl} > 6$ molal). As the activity coefficients of various Cm(III) complexes with stronger ligands are spectroscopically determined (see below) as a function of the brine composition (Cl^- concentration) its effect on the emission spectra has to be known first.

Some selected fluorescence emission spectra taken at different $CaCl_2$ molalities are plotted in Fig. 2. The spectrum at 0 molal $CaCl_2$ represents the aqueous Cm^{3+} ion. When the concentration of $CaCl_2$ is increased up to about 2 mol $CaCl_2$/kg H_2O, the emission spectra show no significant change in position, shape or intensity. At higher $CaCl_2$ concentrations, the spectrum changes systematically with increasing the Cl^- concentration. The peak growing
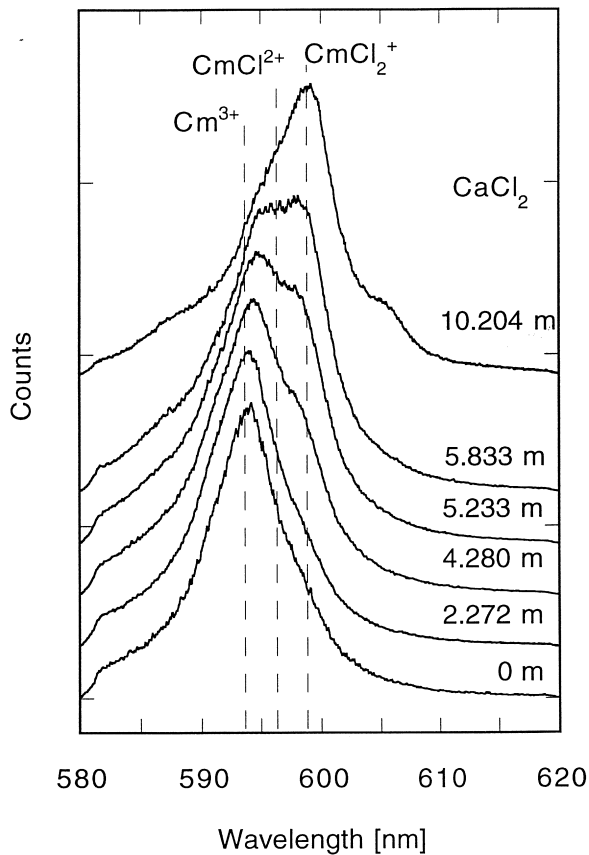
Fig. 2. Selected fluorescence emission spectra of Cm(III) at different CaCl$_2$ molalities.

species distribution is plotted in Fig. 3. The formation of chloro complexes becomes significant only at high chloride concentrations. At $m_{Cl} < 5$ mol/kg H$_2$O, less than 10% of Cm(III) appears to be inner-sphere chloro complexes. Consequently the interaction of Cm(III) with other inorganic ligands can be spectroscopically determined in NaCl solutions up to saturation without invoking the formation of chloro complexes but treating the interaction of Cm^{3+} with Cl$^-$ as strong ion-ion interaction. Only at higher Cl$^-$ concentrations (e.g. in concentrated MgCl$_2$ brines) the formation of chloro complexes has to be considered. A more detailed discussion on Cm(III) chloro complexes is summarized in ref. [16,27].

5.2. Cm(III)-sulfato-complexes

The sulfate ion is another relatively weak ligand with relatively high concentrations in natural brines. Three different sulfato complexes, Cm(SO$_4$)$_n^{3-2n}$ with $n = 1,2,3$ are spectroscopically identified. Selected fluorescence emission spectra of Cm(III) at different sulfate concentrations are given in Fig. 4. To quantify the sulfate complexation equilibria, fluorescence emission spectra are taken in NaCl/Na$_2$SO$_4$ solutions of constant ionic strength (3 molal).

The relatively weak sulfate complexation of Cm(III) necessitates the experiment to be performed at relatively high sulfate concentrations of up to 0.4 molal. The question arises up to which sulfate concentration the activity coefficient quotient (see Eq. (1)) can be considered

at about 598 nm is attributed to the formation of chloride complexes. Up to the CaCl$_2$ molality of about 6 mol/kg H$_2$O, the monochloro and dichloride complexes are identified by peak deconvolution. In a supersaturated CaCl$_2$ solution (10.2 mol/kg H$_2$O) an extra shoulder at about 603 nm appears as can be seen in the upper spectrum in Fig. 2. Under these conditions, one further complex CmCl$_{3(aq)}$ is presumably formed. The experimentally determined

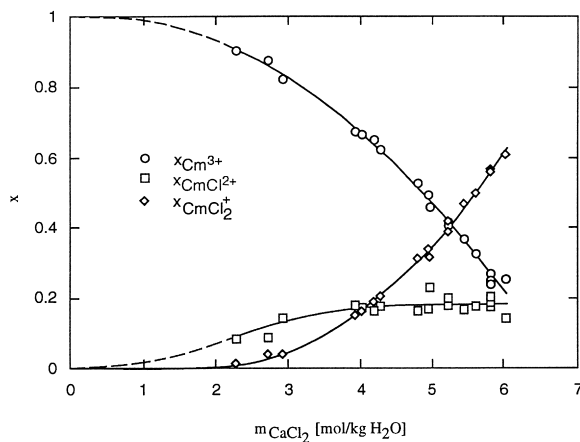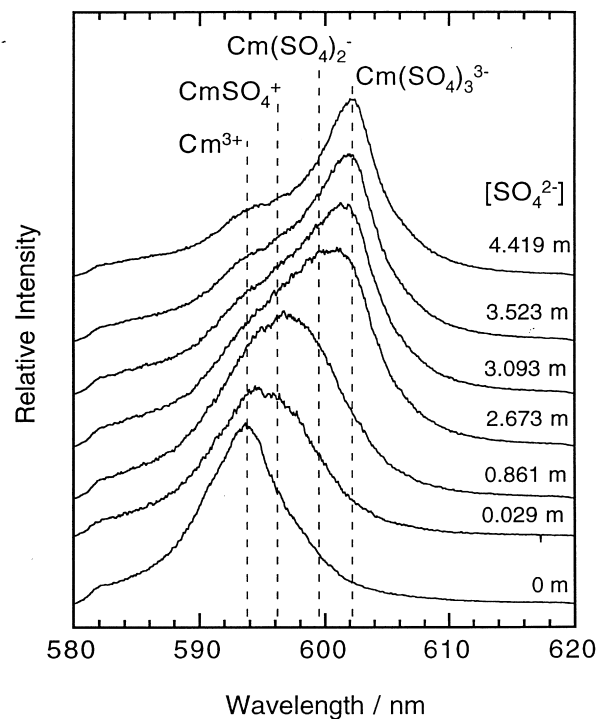Fig. 3. Experimentally determined mole fractions of Cm^{3+}, CmCl^{2+}, and CmCl$_2^+$ as a function of the CaCl$_2$ molality.

Fig. 4. Selected fluorescence emission spectra of Cm(III) at different Cs$_2$SO$_4$ molalities.

as constant at constant ionic strength. Applying the Pitzer ion interaction equations all necessary activity coefficients are calculated as a function of the solution composition. For the formation of $CmSO_4^+$ and $Cm(SO_4)_2^-$, the complexation constants are recalculated taking into account the activity coefficients and plotted in Fig. 5 as dashed lines. At higher sulfate concentrations, a deviation from the straight lines occurs. For the monosulfato complex, the maximum deviation is less than 0.05 logarithmic units and can be neglected. For the disulfato complex, the deviation is about 0.1 logarithmic units, which is in the same region as the estimated experimental error. Hence for sulfate concentrations up to 0.35 molal the activity coefficient quotient can be considered as constant and the constant ionic medium concept is applicable [17].

The time dependence of the Cm(III) fluorescence in various sulfate media follows a monoexponential decay law. The following lifetimes are evaluated for Cm^{3+} and for the sulfato complexes:

$$Cm^{3+}: 65 \pm 2 \mu s; \quad CmSO_4^+: 88 \pm 2 \mu s; \quad Cm(SO_4)_2^-: 95 \pm 8 \mu s;$$

$$Cm(SO_4)_3^{3-}: 195 \pm 8 \mu s;$$

The general trend of the lifetimes is in agreement with the fluorescence intensity factors. While replacing water molecules of the first hydration sphere of the Cm^{3+} ion by sulfate ligands, the quenching caused by the O–H vibration is reduced and hence the lifetime and the fluorescence intensity factor grow with increasing number of sulfate ligands in the complex. A correlation between the reciprocal life times and the number of coordinated water molecules has been calibrated for Cm(III) doped in various lanthanum compounds [25]. Based on this calibration and
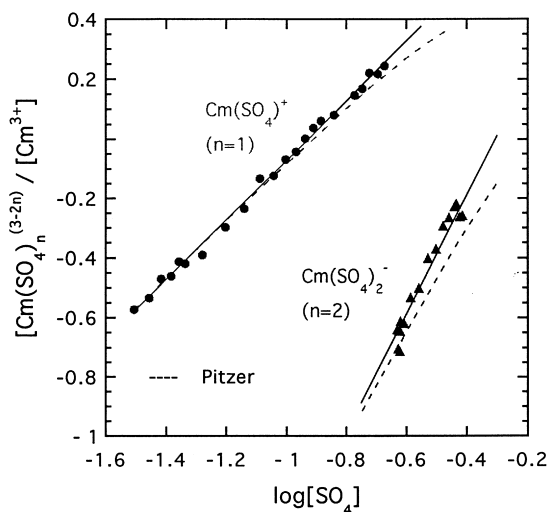
the life times given above, the number of coordinated water molecules are calculated to be:

$$Cm^{3+}: 9.1 \pm 0.6; \quad CmSO_4^+: 6.5 \pm 0.6; \quad Cm(SO_4)_2^-: 5.9 \pm 0.7;$$

$$Cm(SO_4)_3^{3-}: 2.4 \pm 0.5.$$

These values are relatively close to the expected hydration number of Cm(III) complexed with sulfate assuming bidentate coordination of the sulfate ligand.

In natural brine only the monosulfato and partly the disulfato complexes of Cm(III) can be present under certain conditions. The stability constants of those complexes have been determined as a function of the NaCl molality at constant sulfate concentrations as illustrated in Fig. 6 and are used for the parameterization of the ion interaction model. Detailed results on the Cm(III) sulfate complexation are given elsewhere [17,28].

5.3. Cm(III)-hydroxo-complexes

Hydrolysis is one of the most important reactions of trivalent actinides in natural aquatic systems. Experimental results on the Cm(III) hydrolysis are discussed in detail in ref. [15]. Fluorescence emission spectra of Cm(III) taken at constant NaCl molality (2 molal) and at different pH are plotted in Fig. 7. The spectrum at pH 4.68 represents the Cm^{3+} ion. At this pH the hydrolysis can be neglected. With increasing pH the fraction of the hydroxo species $CmOH^{2+}$ and $Cm(OH)_2^+$ increases. The decreasing intensity of the spectra with increasing pH correlates with the decrease of the total curium concentration caused by surface sorption. The mole fractions of different species are deduced from the spectra by peak deconvolution. A typical example is illustrated in Fig. 8. In the upper part of
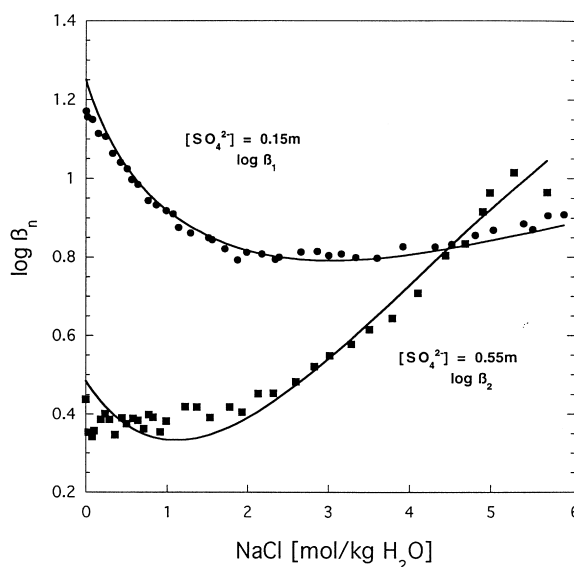

Fig. 5. Correlation of the experimentally determined ratio $[Cm(SO_4)_n^{(3-2n)}]/[Cm^{3+}]$ with the SO_4^{2-} molality in the logarithmic scale ($n = 1, 2$). The solid lines are calculated assuming theoretical slopes 1 and 2, respectively; the dashed lines are calculated with the Pitzer approach (see text).

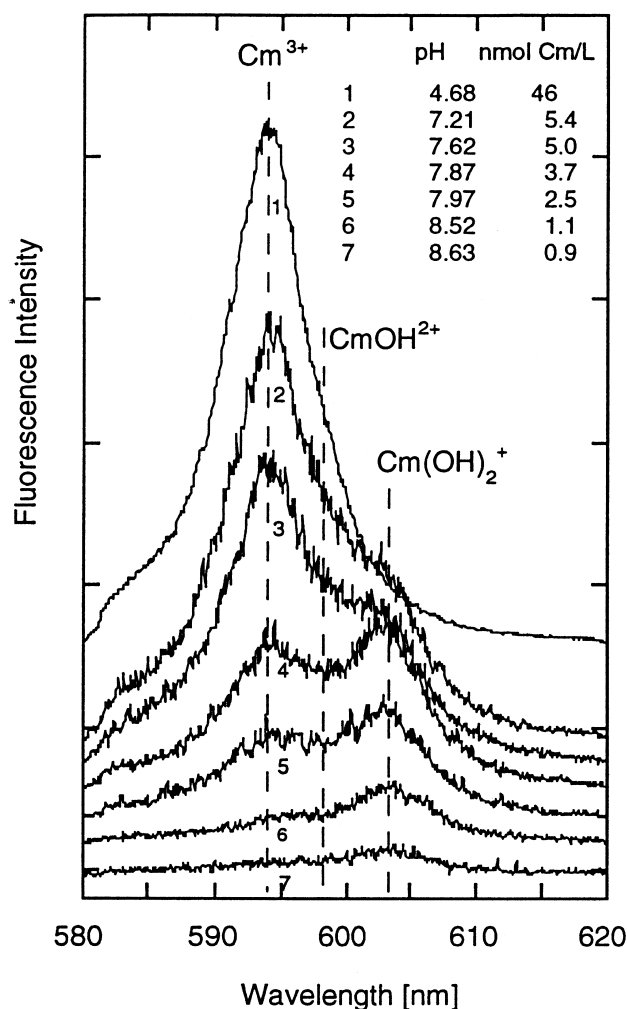Fig. 6. The sulfate complex formation constants β_1 and β_2 of Cm(III) as a function of the NaCl molality.

Fig. 7. Selected fluorescence emission spectra at different pH and at constant NaCl molality (2 molal).

Fig. 8. Peak deconvolution of a mixed spectrum.

Fig. 8, the measured spectrum and the spectra of individual components are plotted, each multiplied with an appropriate factor. The lower part of Fig. 8 shows the difference between the measured spectrum and the summed up spectrum of individual components.

The dependence of the first and second hydrolysis constants on the NaCl molality from diluted up to saturated NaCl solutions is plotted in Fig. 9. The data are used to parameterize the Pitzer approach. Both curves show a minimum at about 0.5 mol NaCl/kg H_2O. At high NaCl molalities, in particular, the second hydrolysis constant increases more than two orders of magnitude.

5.4. Cm(III)-carbonato-complexes

The carbonate ion forms strong complexes with trivalent actinides. As carbonate is always present under natural aquatic conditions, the carbonate complexation is one of the most important geochemical reactions of actinides in natural aquat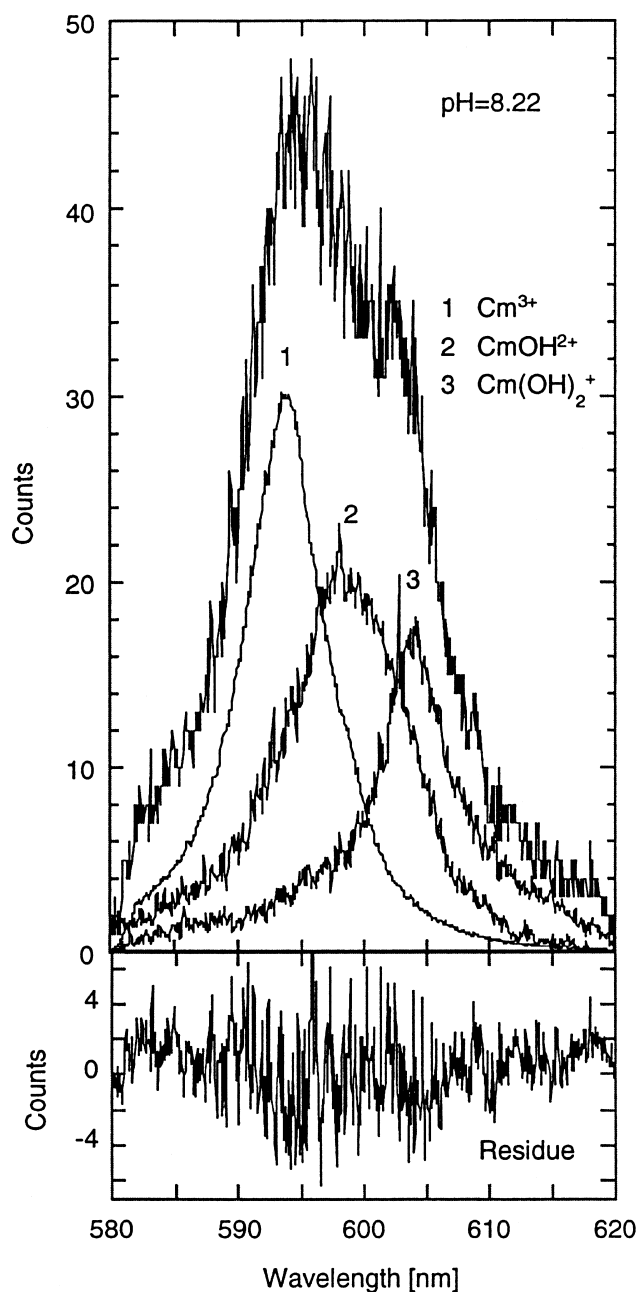ic systems. The carbonate complexation of Cm(III) is investigated in constant ionic strength NaCl solution (1 molal) varying the carbonate concentration over a wide range. A detailed discussion on carbonate complexation is given in ref. [29]. Selected spectra are presented in Fig. 10. Fig. 10a contains spectra measured at low carbonate concentrations ($[CO_3^{2-}] < 10^{-4}$ molal) and low pH (pH<7), while in Fig. 10b results of batch experiments ($[CO_3^{2-}] > 10^{-4}$ molal; pH>8) are presented. The carbonate complexes $CmCO_3^+$, $Cm(CO_3)_2^-$ and $Cm(CO_3)_3^{3-}$ are quantified spectroscopically by peak deconvolution of fluorescence emission spectra.

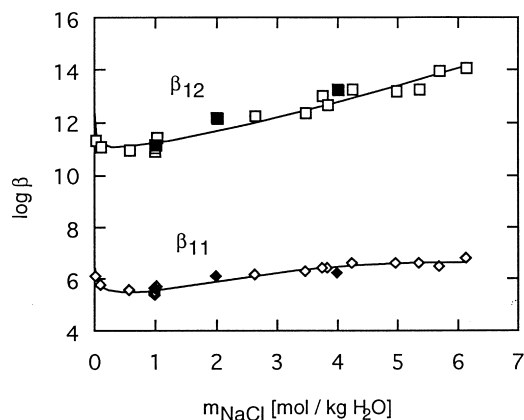At high CO_2 partial pressure (>500 mbar) and pH<6.5,

Fig. 9. The first and second hydrolysis constants of Cm(III) as a function of the NaCl molality. Open symbols, experiments at constant pH; solid symbols, experiments at constant NaCl molality and various pH.

there is evidence for the formation of Cm(III) bicarbonate complexes to a small extent. Our initial intention to evaluate the spectroscopic data by taking into account only carbonate complexes $Cm(CO_3)_n^{3-2n}$ failed. Therefore, it is concluded that at low pH and high CO_2 partial pressure, besides carbonate complexes, a bicarbonate complex can be stable. The complexation constant for $CmHCO_3^{2+}$ is found to be $\log \beta = 1.9 \pm 0.2$ in 1 molal NaCl. In order to prove spectroscopically whether a bicarbonate complex is stable, spectroscopic investigation with TRLFS is performed in 1 molal NaCl at elevated CO_2 pressures of 11

bar at room temperature in a special high pressure cell. The experiments, performed under conditions (pH about 4.4) where the carbonate complexation can be neglected ($[CO_3^{2-}] < 10^{-7}$) prove the presence of the postulated $CmHCO_3^{2+}$ complex [26].

In our experimental results there is no indication for the formation of mixed hydroxo carbonato complexes. Emission spectra at constant carbonate concentrations appears independent of pH. At very high carbonate concentrations (>0.1 molal) an additional complex is identified. The experimental data indicate that under these conditions the tetracarbonato complex is formed. Although, to our knowledge, the tetracarbonato complexes have not yet been confirmed for trivalent actinides, its formation is reported for trivalent lanthanides, e.g. europium [30] and cerium [31]. The complexation constants are comparable to the values determined for Cm(III).

The ionic strength dependence of the complexation equilibria is determined in solutions of nearly constant carbonate concentration with varying the NaCl concentration over a wide range up to saturation. The apparent stability constants for $CmCO_3^+$, $Cm(CO_3)_2^-$, $Cm(CO_3)_3^{3-}$ and $Cm(CO_3)_4^{5-}$ are determined at each given NaCl molality. The experimental results are summarized in Fig. 11. Based on this result the ion-interaction approach (Pitzer equation) is parameterized [32]. There is a considerable increase of the complexation constants of the complexes $Cm(CO_3)_3^{3-}$ and $Cm(CO_3)_4^{5-}$ at high NaCl
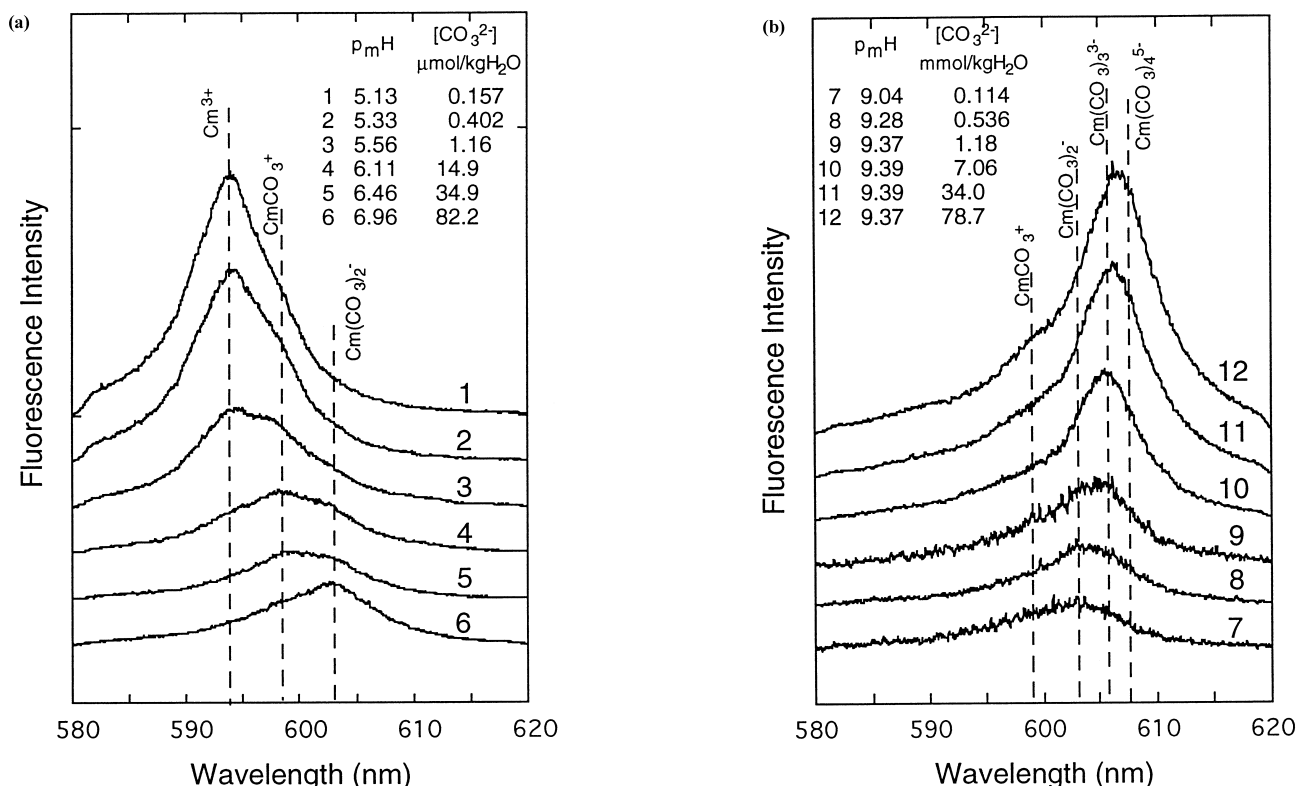

Fig. 10. Selected fluorescence emission spectra at different carbonate concentrations. (a) $pmH < 7$; $[CO_3^{2-}] < 10^{-4}$ m; (b) $pmH > 8$; $[CO_3^{2-}] > 10^{-4}$ m.

Table 1
Thermodynamic equilibrium constants and Pitzer ion-interaction parameters for trivalent actinides at 25°C

	$\log K^0$			Ref.
Thermodynamic constants				
$H_2O \rightleftharpoons H^+ + OH^-$	-13.997			[35]
$CO_{2(g)} \rightleftharpoons CO_2^0$	-1.482			[35]
$H_2O + CO_2^0 \rightleftharpoons H^+ + HCO_3^-$	-6.337			[35]
$HCO_3^- \rightleftharpoons H^+ + CO_3^{2-}$	-10.339			[35]
$Cm^{3+} + Cl^- \rightleftharpoons CmCl^{2+}$	0.24			[27]
$Cm^{3+} + 2Cl^- \rightleftharpoons CmCl_2^+$	-0.74			[27]
$Cm^{3+} + OH^- \rightleftharpoons CmOH^{2+}$	6.44			[27]
$Cm^{3+} + 2OH^- \rightleftharpoons Cm(OH)_2^+$	12.30			[27]
$Cm^{3+} + SO_4^{2-} \rightleftharpoons CmSO_4^+$	3.25			[28]
$Cm^{3+} + 2SO_4^{2-} \rightleftharpoons Cm(SO_4)_2^-$	3.70			[28]
$Cm^{3+} + CO_3^{2-} \rightleftharpoons CmCO_3^+$	8.10			[32]
$Cm^{3+} + 2CO_3^{2-} \rightleftharpoons Cm(CO_3)_2^-$	13.0			[32]
$Cm^{3+} + 3CO_3^{2-} \rightleftharpoons Cm(CO_3)_3^{3-}$	15.2			[32]
$Cm^{3+} + 4CO_3^{2-} \rightleftharpoons Cm(CO_3)_4^{5-}$	13.0			[32]

Binary interaction parameters	$\beta^{(0)}$	$\beta^{(1)}$	C^ϕ	
H^+/Cl^-	0.1775	0.2945	0.0008	[35]
Na^+/Cl^-	0.0765	0.2664	0.00127	[35]
Na^+/SO_4^{2-}	0.01958	1.113	0.00497	[35]
Na^+/HCO_3^-	0.0277	0.0411	0.0	[35]
Na^+/CO_3^{2-}	0.0399	1.389	0.0044	[35]
Na^+/OH^-	0.0864	0.253	0.0044	[35]
Cm^{3+}/Cl^-	0.5856	5.6	-0.0166	[27]
$CmCl^{2+}/Cl^-$	0.593	3.15	-0.006	[27]
$CmCl_2^+/Cl^-$	0.516	1.75	0.010	[27]
$CmOH^{2+}/Cl^-$	-0.055	1.6	0.050	[27]
$Cm(OH)_2^+/Cl^-$	-0.616	-0.45	0.050	[27]
Cm^{3+}/SO_4^{2-}	1.792	15.04	0.600	[28]
$CmSO_4^+/Cl^-$	-0.091	-0.39	0.048	[28]
$Na^+/Cm(SO_4)_2^-$	-0.354	0.40	0.051	[28]
$CmCO_3^+/Cl^-$	-0.072	0.403	0.0388	[32]
$Na^+/Cm(CO_3)_2^-$	-0.240	0.224	0.0284	[32]
$Na^+/Cm(CO_3)_3^{3-}$	0.125	4.730	0.0007	[32]
$Na^+/Cm(CO_3)_4^{5-}$	2.022	19.22	-0.305	[32]

	λ		
$Na^+/Cm(OH)_3^0$	-0.2		[27]
$Cl^-/Cm(OH)_3^0$	-0.2		[27]
Na^+/CO_2^0	0.1		[35]
Cl^-/CO_2^0	-0.005		[35]

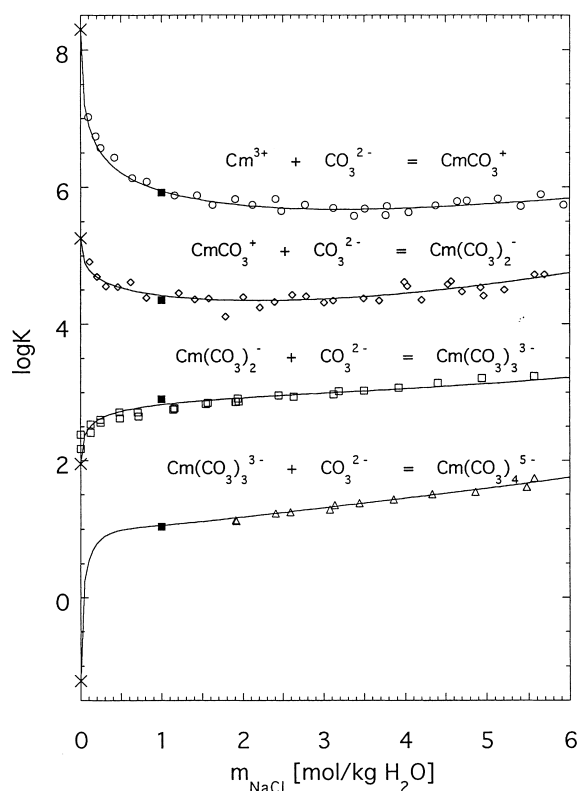| **Ternary interaction parameters**			
i/j/k	Θ_{ij}	ψ_{ijk}	
$H^+/Na^+/Cl^-$	0.036	-0.004	[35]
$Na^+/Cl^-/SO_4^{2-}$	0.02	0.0014	[35]
$OH^-/Cl^-/Na^+$	-0.05	-0.006	[35]
$OH^-/CO_3^{2-}/Na^+$	0.1	-0.017	[35]
$HCO_3^-/Cl^-/Na^+$	0.03	-0.015	[35]
$HCO_3^-/CO_3^{2-}/Na^+$	-0.04	0.002	[35]
$CO_3^{2-}/Cl^-/Na^+$	-0.02	0.0085	[35]
$Na^+/Cm^{3+}/Cl^-$	0.1	0.0	[27]
$Ca^{2+}/Cm^{3+}/Cl^-$	0.2	0.0	[27]
$Ca^{2+}/CmCl^{2+}/Cl^-$	-0.014	0.0	[27]
$Ca^{2+}/CmCl_2^+/Cl^-$	-0.196	0.0	[27]

Fig. 11. The carbonate complexation constants as a function of the NaCl molality.

molalities. As expected, these complexes with high negative charge are stabilized by the large excess of positively charged Na^+ ions.

In natural brines the hydroxo and the carbonato complexes are the most stable aqueous complexes, while the sulfato and in particular the chloro complexes are very weak. However, in brines the concentrations of SO_4^{2-} and Cl^- can be very high and therefore complexes with these ligands can be important in particular in $MgCl_2$ brines with acid pH. We have therefore placed our emphasis on these four ligands. Cm(III) complexes with other ligands, e.g. F^-, $H_2PO_4^-$ and $H_3SiO_4^-$, have not yet been investigated in brines. Although their complexation constants are relatively high (in 0.1 M $NaClO_4$) their concentration is usually very low in natural brines. Hence they are expected to be of minor importance in natural brines.

5.5. Thermodynamic model for trivalent actinides

Based on the spectroscopic results (apparent stability constants as a function of the NaCl $(CaCl_2)$-molality; see Fig. 3, Fig. 6, Fig. 9, Fig. 11) the ion interaction parameters for the Cm(III) species and a set of thermodynamic complexation constants (chemical potentials) at zero ionic strength are evaluated (Table 1). As natural brines are multicomponent electrolyte solutions of high ionic strength, the ion-interaction (Pitzer) approach [21] is

applied for calculating the activity coefficients of various Cm(III) species. While the ion-interaction parameters of the five component sea water system Na-K-Mg-Cl-SO₄-H_2O are known [33] there is very little information available on the interaction parameters of trivalent actinides species. As the Cm(III) species are trace components ($m < 10^{-6}$ mol/kg H_2O) their activity coefficients depend on the concentration of the main components only and are independent of the concentration of other trace species in the system. The available experimental data do not allow to evaluate all unknown ion-interaction parameters. Only those parameters having considerable influence on activity coefficients of trace Cm(III) species have been determined. These are mainly the parameters accounting for the interaction of Cm(III) species with the main counter ion. For positively charged Cm(III) species the interaction with Cl^- and in some cases with SO_4^{2-} and for negatively charged Cm(III) with Na^+ are considered. Mixing parameters of Cm(III) species are in general neglected, only in a few cases it is necessary to estimate parameters accounting for the interaction of ions of the same sign. Details on the evaluation of the Pitzer parameters are given in our previous publications [15,27,28,32].

For modeling the thermodynamics of trivalent actinides, an oxidation state analogy is applied. The interaction of the trivalent actinides, Cm(III), Am(III), Pu(III) and of Nd(III), with counter ions of the main components of the system are assumed to be the same for each corresponding species. The derived thermodynamic model is tested by comparing model predictions with independent experimental data. As an example the solubility of $Am(OH)_3(s)$ in 5.61 molal NaCl solutions is calculated as function of the pmH (pmH = log m_{H^+}) and the results are compared to experimental data [34]. The thermodynamic solubility
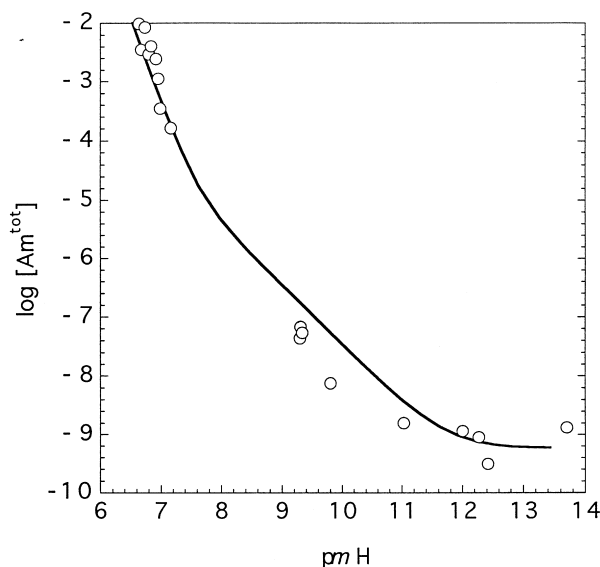

Fig. 12. Solubility of $Am(OH)_3(s)$ in 5.61 molal NaCl solutions as a function of pmH. ○, [34] — calculated with ion interaction approach.

product of Am(OH)$_3$(s) log $K°$sp $= -27.5$ [35] is used for the calculation. As illustrated in Fig. 12 the calculated solubilities agree fairly well with the experimental data.

6. Conclusion

A model capable of predicting the thermodynamic properties of trivalent actinides in high concentrated brines has been developed based on spectroscopic experiments. The model is based on the ion-interaction approach (Pitzer equations) considering the interaction of stable inorganic complexes (carbonato, hydroxo, sulfato and chloro) of trivalent actinides with the main brine components. The model is valid from low to high salt concentrations.

References

[1] N. Edelstein, J. Bucher, R. Silva, H. Nitsche, Report ONWI-399 and LBL-14325, Lawrence Berkley Laboratory, Berkley, CA, 1983.

[2] D. Rai, R.G. Strickert, D.A. Moore, J.L. Ryan, Radiochim. Acta 33 (1983) 201.

[3] J.I. Kim, M. Bernkopf, Ch. Lierse, F. Koppold, ACS Symposium Series, no. 246, American Chemical Society, Washington, DC, 1984, pp. 115–134.

[4] S. Stadler, J.I. Kim, Radiochim. Acta 44–45 (1988) 39.

[5] G. Meinrath, J.I. Kim, Radiochim. Acta 52–53 (1991) 29.

[6] W. Runde, G. Meinrath, J.I. Kim, Radiochim. Acta 58–59 (1992) 93.

[7] E. Giffaut, P. Vitorge, Mater. Res. Soc. Symp. Proc. 294 (1993) 747.

[8] G.R. Choppin, R.C. De Carvalho, J. Inorg. Nucl. Chem. 29 (1967) 725.

[9] G.R. Choppin, R.C. De Carvalho, J. Inorg. Nucl. Chem. 29 (1967) 737.

[10] H. Nitsche, E.M. Standifer, R.J. Silva, Radiochim Acta 46 (1989) 185.

[11] R.J. Silva, G. Bidoglio, M.H. Rand, P.B. Robouch, H. Wanner, I. Puigdomenech, Chemical Thermodynamics of Americium, Elsevier, 1995.

[12] J. Fuger, I.L. Khodakovsky, E.I. Sergeyeva, V.A. Medvedev, J.D. Navratil, The Chemical Thermodynamics of Actinide Elements and Compounds, Part 12, The Actinide Aqueous Inorganic Complexes, IAEA, Vienna, 1992.

[13] H. Wimmer, R. Klenze, J.I. Kim, Radiochim. Acta 56 (1992) 79.

[14] J.I. Kim, R. Klenze, H. Wimmer, W. Runde, W. Hauser, J. Alloys Comp. 213–214 (1994) 333.

[15] Th. Fanghänel, J.I. Kim, P. Paviet, R. Klenze, W. Hauser, Radiochim. Acta 66–67 (1994) 81.

[16] Th. Fanghänel, J.I. Kim, R. Klenze, Y. Kato, J. Alloys Comp. 225 (1995) 308.

[17] P. Paviet, Th. Fanghänel, R. Klenze, J.I. Kim, Radiochim. Acta 74 (1996) 99.

[18] J.I. Kim, R. Stumpe, R. Klenze, Topics in Current Chemistry, vol. 157, Springer-Verlag, Berlin, Heidelberg, 1990, pp. 129–179.

[19] J.V. Beitz, J.P. Hessler, Nucl. Techn. 51 (1980) 169.

[20] J.I. Kim, R. Klenze, H. Wimmer, Eur. J. Solid State Inorg. Chem. 28 (1991) 347.

[21] K.S. Pitzer, Activity Coefficients in Electrolyte Solutions, 2nd ed., CRC Press, Boca Raton, 1991.

[22] W.T. Carnall, K. Rajnak, J. Chem. Phys. 63 (1975) 3510.

[23] W.T. Carnall, H.M. Crosswhite, Report ANL-84-90, 1995.

[24] J.V. Beitz, D.L. Bowers, M.M. Doxtader, V.A. Maroni, D.T. Reed, Radiochim. Acta 44–45 (1988) 87.

[25] T. Kimura, G.R. Choppin, J. Alloys Comp. 213–214 (1994) 313.

[26] Th. Fanghänel, H.T. Weger, G. Schubert, J.I. Kim, Radiochim. Acta (accepted).

[27] Th. Könnecke, Th. Fanghänel, J.I. Kim, Radiochim. Acta 76 (1997) 131.

[28] Th. Könnecke, P. Paviet-Hartmann, Th. Fanghänel, J.I. Kim, Radiochim. Acta, to be published.

[29] Th. Fanghänel, H.T. Weger, Th. Könnecke, V. Neck, P. Paviet-Hartmannn, E. Steinle, J.I. Kim, Radiochim. Acta (accepted).

[30] R.R. Rao, A. Chatt, Radiochim. Acta 54 (1991) 181.

[31] D. Ferri, I. Grenthe, S. Hietanen, F. Salvatore, Acta Chim. Scand. A37 (1983) 359.

[32] Th. Fanghänel, Th. Könnecke, H.T. Weger, P. Paviet- Hartmann, V. Neck, J.I. Kim, Radiochim. Acta, to be published.

[33] C.E. Harvie, N. Moller, J.H. Weare, Geochim. Cosmochim. Acta 48 (1984) 723.

[34] W. Runde, J.I. Kim, RMC-01094, Institut für Radiochemie, Technische Universität München, 1994.

[35] L.R. Morss, C.W. Williams, Radiochim. Acta 66–67 (1994) 89.